Generation of higher-order optical (2+1)-dimensional spatial vector solitons in a nonlinear anisotropic medium

Carsten Weilnau* and Cornelia Denz
Institute of Applied Physics, Westfälische Wilhelms-Universität Münster, Corrensstrasse 2-4, D-48149 Münster, Germany

Marcus Ahles, Andreas Stepken, Kristian Motzek, and Friedemann Kaiser
Institute of Applied Physics, Darmstadt University of Technology, Hochschulstrasse 4-6, D-64289 Darmstadt, Germany
(Received 23 May 2001; published 9 October 2001)

We investigate the generation of higher-order optical vector solitons in two transverse dimensions in anisotropic nonlinear media consisting of an incoherent superposition of a Gaussian beam and a higher-order laser mode with a complex internal modal structure. We demonstrate both numerically and experimentally various examples of these stable self-trapped light structures and show that vortex modes carrying topological charge always decay into multiple-humped structures that remain self trapped during propagation. Furthermore, we demonstrate the mutual stabilization of a triple- and a double-humped transverse light structure leading to the formation of a two-dimensional vector soliton without a stabilizing fundamental Gaussian mode.

DOI: 10.1103/PhysRevE.64.056601 PACS number(s): 42.65.Tg, 05.45.Yv, 42.65.Hw

I. INTRODUCTION

Stable self focusing of light in a medium with a saturable Kerr-type nonlinearity has attracted much research interest within the last decade [1]. A monochromatic and highly coherent light beam propagating in a saturable nonlinear material induces a refractive index modulation that counterbalances the natural diffraction. Therefore, the beam remains self trapped and propagates as the fundamental mode of its self-induced waveguide. These self-focused light structures that consist of only one optical field are denoted as scalar solitons. In contrast, vector solitons are self-trapped optical beams that consist of more than one optical field. They were first suggested by Manakov [2] for the case of a Kerr nonlinearity and two beams of different polarization states [3]. Here, at least two copropagating beams interact via the nonlinear response of the material and jointly induce a multimode waveguide in which they propagate as eigenmodes [4]. It is essential for the formation of all kinds of vector solitons that the interference between the individual components must not contribute to the induced refractive index change Δn, and therefore, it has to be destroyed. For this purpose it is convenient to use mutually incoherent components.

Optical spatial vector solitons have been extensively analyzed in the planar $(1+1)$-dimensional (D) geometry in media with a Kerr-like saturable optical nonlinearity. Various combinations of a fundamental single-humped and a double-humped beam were observed experimentally [5] and studied theoretically [6]. Further on, collision-induced shape transformation [7] as well as energy exchange upon collision [8] of these soliton pairs have been reported. Recently, the existence of multicomponent solitary waves in two transverse dimensions has been predicted on the basis of a saturable and isotropic model [9,10] and subsequently has been observed in experiments [11,12]. They consist of one bell-shaped Gaussian beam and a second beam bearing a higher-order laser mode of Hermite-Gaussian (HG) or Laguerre-Gaussian (LG) type. Among various possible configurations it is particularly the HG_{01}-like dipole mode that allows the generation of a very robust type of optical spatial vector soliton; the dipole-mode vector soliton. In contrast, all combinations of a fundamental Gaussian mode and a LG_{01}-modelike vortex carrying topological charge ($m=1$) are linearly unstable and decay into a stable dipole-mode structure carrying angular momentum [10,11]. The robustness of the dipole-mode vector soliton motivates the investigations on higher-order multihumped solitary waves. Multihumped self-trapped optical beams have only been realized in the planar $(1+1)$D geometry so far [5] and a numerical stability analysis revealed that combinations consisting of higher-order modes such as triple-humped transverse light structures are linearly unstable [6]. The instability that leads to a breakup of the combined structures becomes dominant at large propagation distances and was therefore not observed experimentally. Previous theoretical investigations that describe the formation of vector solitons in photorefractive crystals are based on saturable and isotropic nonlinear models [9,10]. However, the photorefractive nonlinearity is of anisotropic nature [13] and therefore, the experimental results deviate from numerical simulations. Here, we present a numerical analysis of vector solitons in bulk anisotropic medium. It is particularly the nonlocal nature of the anisotropic refractive index change in a DC-electric field biased strontium barium niobate (SBN) photorefractive crystal that supports the formation of these multicomponent solitary waves with an elaborate geometry. Moreover, we demonstrate experimentally and numerically the existence of composite solitons consisting of higher-order modes.

Our contribution is divided into three main parts. First, we demonstrate that the incoherent combination of a Gaussian and a vortex beam with a topological charge of $m=2$ does not form a stable self-trapped structure but decays via an intermediate state consisting of two single-charged vortices into a triple-humped structure (THS). Second, we show that the structure, consisting of a triple-humped higher-order mode and a fundamental Gaussian mode, propagates self consistently in the nonlinear material and forms a triple-

*Electronic mail: weilnau@uni-muenster.de

humped vector soliton. Finally, we demonstrate the mutual stabilization of a double-humped and a triple-humped component that results in the formation of a localized optical light structure even without the fundamental Gaussian component. It is indeed surprising that the combination of two unstable components leads to the formation of a self-trapped state. Therefore, the presence of the stabilizing fundamental Gaussian beam is not a general requirement to generate optical spatial vector solitons in two transverse dimensions.

II. EXPERIMENT

The experimental setup for the generation of optical vector solitons consisting of two components is similar to the one that was earlier described in [11]. We derive two beams from a frequency-doubled Nd:YAG-laser ($\lambda = 532$ nm) with the help of a Mach-Zehnder-like configuration. One of the beams is transmitted through a phase mask to get the required transversal profile for the higher-order mode in the first diffraction order. The second Gaussian beam is reflected by a mirror mounted on a piezoelectric device that oscillates at about 1 kHz before it is recombined with the first beam bearing the higher-order mode. Due to the crystal's noninstantaneous response it cannot follow the interference fluctuations induced by the fast oscillating mirror. With this technique, we obtain two effectively incoherent but copropagating optical beams that will become the constituents of the higher-order vector soliton. Finally they are focused onto the front face of a cerium-doped (0.002% wt.) SBN:60 crystal with dimensions of $13.5\times5\times5$ mm^3, $(a\times b\times c)$. The beam spot size at the crystal front face is about 12 μm full width at half maximum. They propagate either along the crystal's a or b axis that corresponds to a propagation length of 5 or 13.5 mm, respectively. The crystal is biased with a DC-electric field of 1.5–2 kV along its c axis in order to use the large r_{33} electro-optic coefficient of SBN. Additionally, the crystal is illuminated with incoherent white light to control the degree of saturation of the nonlinearity that is in the range of unity for all our experiments. Finally, we image the crystal's front and exit face on a charge-coupled device camera connected to a computer system. Due to the slow response of our material, we are able to resolve the single constituents of the multicomponent beam by blocking one component and recording the remaining light intensity from the other constituent within a short time interval of ($\Delta\tau \approx 0.1$ s).

A. Experimental results

First, we investigate the copropagation of an optical vortex with topological charge $m=2$ and a fundamental Gaussian component. The vortex beam with a total power of $P_v = 1.6$ μW is formed by diffraction of a light beam from a computer-generated hologram and is incoherently combined with the Gaussian beam of nearly equal total power $P_G = 1.8$ μW. Both beams overlap completely while propagating 13.5 mm through the nonlinear material. Figure 1(a) shows the input intensity distribution for the vortex component (upper row) and the Gaussian component (bottom row).

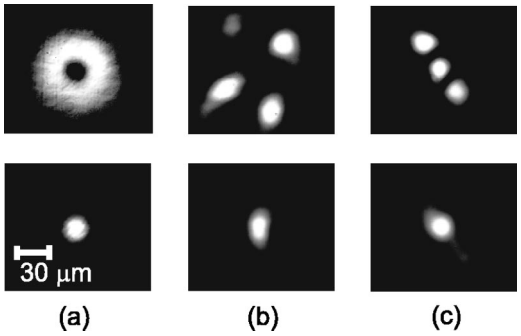

FIG. 1. Decay of a vortex ($m=2$) in the presence of a Gaussian beam. The vortex and Gaussian component are shown in the upper and bottom row, respectively. Intensity distribution at the input face (a), and exit face of the crystal for a separate propagation (b) and a combined propagation (c) of 13.5 mm with 1.9 kV applied along the c axis.

Figures 1(b) illustrate the crystal's exit face for the case when each beam propagates separately in the biased nonlinear medium. The double-charged vortex, which has a screw-like transversal phase distribution does not form a self-focused state, it merely disintegrates into three quasisolitons that arrange in a triangular way [Fig. 1(b), top]. This breakup behavior is somehow similar to the theoretical investigations given in [14]. In contrast, the Gaussian beam remains self trapped and forms an ordinary elliptically shaped photorefractive soliton [Fig. 1(b), bottom]. The situation changes completely when both beams copropagate incoherently in the medium, as depicted in Fig. 1(c). The vortex disintegrates now into three well-defined spots that rearrange along a line that is tilted with respect to the vertical axis by 33° [Fig. 1(c), top]. The fundamental Gaussian component basically remains in its shape and becomes slightly elongated in the direction of the triple-humped structure.

To get a deeper insight into the processes taking place in the crystal during the propagation of the two beams, we flip the sample by 90° and use its 5-mm long b axis for our investigations, which displays equal nonlinear properties. With an external voltage of 1.8 kV and beam powers of $P_v = 1.7$ μW and $P_G = 1.9$ μW, the boundary conditions are nearly unchanged. Figure 2(a) illustrates the vortex component after 5 mm simultaneous propagation with the fundamental beam. It does not yet disintegrate into several beamlets but retains its initial donutlike shape and just shows some irregularities that stem from the growing instability during propagation. Via interference with a mutually coherent plane wave we record the interference pattern and thereby visualize the vortex' phase distribution that is illustrated magnified in Fig. 2(b). We clearly identify two single-charged vortices at the position of the two dark spots in Fig. 2(a) with their phase dislocation indicated by the arrows in Fig. 2(b). It shows that a higher-order vortex of charge $m=n$ is topologically unstable and decays into n vortices with charge $m=1$. This was earlier demonstrated in [15] for the case of a defocusing nonlinearity and is in fact a general property of optical beams carrying topological charge even in a linear medium.

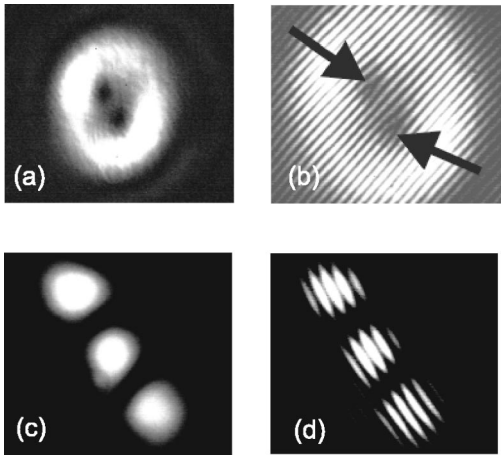

FIG. 2. Decay of a vortex ($m=2$) in the presence of a Gaussian beam. The vortex component after a propagation of 5 mm (a) and 13.5 mm (c) with the according plane-wave interference (b) and (d).

Figure 2(c) illustrates once again the higher-order component of the vector soliton demonstrated in Fig. 1 and the appropriate interference pattern with a plane wave after a propagation of 13.5 mm [Fig. 2(d)]. It clearly shows that the resulting fringes that appear at the location of the three spots are all shifted by π. This demonstrates that the initial phase dislocation of the double-charged vortex transforms first into two closely separated single-charged vortices that then subsequently induce two transversal phase shifts of π and form a triple-humped structure. The subsequent transition from a modulated donut-shaped structure in Fig. 2(a) into a triple-peak structure depicted in Fig. 2(c) is a characteristic feature for the propagation of double-charged optical vortices in saturable self-focusing medium, and was already observed in atomic vapor [16]. In such a system, the single steps of the transition could be visualized by increasing the strength of the nonlinear effect continuously. If the nonlinearity is weak, which is comparable to short propagation distances, the vortex disintegrates and forms two bright spots located on opposite sides of the initial donut. Enhancing the strength of the nonlinear effect, the two lobes start to attract each other and rotate about their common axis and a central peak will be generated. Due to the inherent phase singularities, the single lobes will not fuse but start to repel mutually and separate from each other. Experiments in the isotropic atomic vapor displayed a continuous helical motion of the three beamlets due to a nonvanishing angular momentum carried by the initial vortex beam. In contrast, the anisotropic photorefractive nonlinear system does not support a spiraling motion of the single lobes due to its symmetry-breaking property. Nevertheless, the transverse angular momentum of the vortex component does not vanish but induces an oscillation of the triple-peak structure in the transverse plane. This phenomenon seems to be a generic feature of anisotropic systems, since the interaction of two scalar solitons supports a continuous spiraling motion for an isotropic model [17] and an oscillating motion for the anisotropic model [18].

So far, we have shown that a vector soliton consisting of a double-charged optical vortex in one component and a fundamental Gaussian beam in the second component is unstable and decays into a triple-humped structure during propagation.

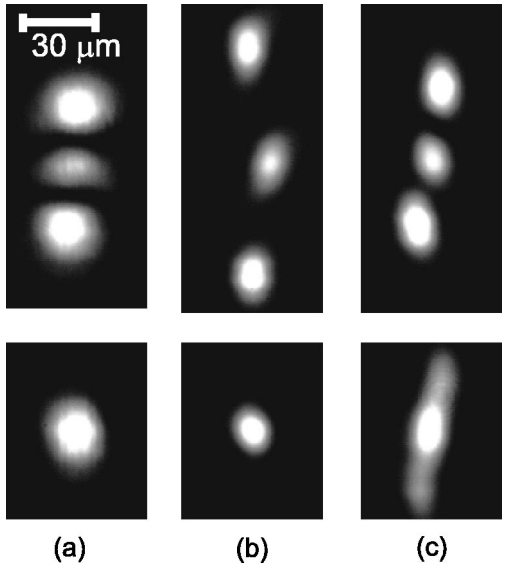

FIG. 3. Stabilization of a triple-humped beam (upper row) in the presence of the Gaussian fundamental mode (bottom row). (a) input intensity. Intensity distribution after 13.5 mm separate (b) and simultaneous (c) propagation.

Now, the nontrivial question arises whether such a THS represents one component of a stable vector soliton. For this purpose, we implement a second experiment where we produce such a triple-humped beam directly and combine it with a fundamental Gaussian beam in the nonlinear medium. We modify the experimental setup and derive four separate beams from our laser source. After being reflected from piezomounted mirrors, they are recombined by several beam splitters and focused onto the front face of the crystal. Three mutually coherent beams are aligned parallel in the direction perpendicular to the crystal's c axis forming the triple-humped higher-order mode. The relative phase of these peaks is shifted by π, which is controlled by piezomechanical drivers. The remaining fourth beam bearing the fundamental Gaussian mode gets effectively incoherent relative to the higher-order component by the reflection from the oscillating mirror, a technique that has been already used in the experiment described above. The result of this investigation is depicted in Fig. 3.

The upper row demonstrates the higher-order, HG_{02}-like component whereas the fundamental mode is represented in the bottom row. Figures 3(a) illustrate the input intensity of the two components with equal total beam power of $P_{\mathrm{THS}}=P_{\mathrm{Gauss}}=1.9\ \mu$W. Figures 3(b) show the evolution of the two beams propagating separately over a distance of 13.5 mm in the crystal biased with 1.8 kV. The lobes of the higher-order component propagate in a self-focused way through the nonlinear material. The refractive index change in between the bright spots is much smaller than in the illuminated areas because of the π-phase shift between adjacent lobes. As a consequence, light will only be attracted in the bright beamlets that therefore appear to repel each other [Fig. 3(b), top]. For example, they experience a ''*repulsive force*,''

whereas the Gaussian component forms an ordinary elliptically shaped photorefractive soliton [Fig. 3(b), bottom]. In the case when both components are present, the three peaks of the THS remain self trapped during the propagation and leave the crystal nearly unchanged compared to the input intensity distribution, as depicted in Fig. 3(c). It is obvious that the Gaussian component stabilizes the whole structure and prevents the single beamlets of the THS from separation during propagation. We conclude that the copropagating higher-order mode and the fundamental Gaussian beam form indeed a triple-humped vector soliton in a photorefractive nonlinear medium. Both components induce a multimode waveguide in which they propagate as eigenmodes. It is essential to mention here that the THS is not just guided by the waveguide induced by the fundamental component, because both beams are of comparable total power and induce therefore a joint refractive index modulation in which they both propagate self consistently. Even though some parts of the THS are not overlapping with the Gaussian component initially, they experience a strong attraction that is due to the nonlocal change of the refractive index induced by the Gaussian beam. Consequently, the shape of the fundamental Gaussian component gets affected in the same way by the presence of the THS and becomes stretched in the vertical direction [Fig. 3(c), bottom]. It is interesting to note that the three lobes of the separately propagating THS depicted in Fig. 3(b) have slightly different intensity and do not align properly along a vertical axis. This effect can be understood in terms of the diffusion-dominated charge-carrier transport process that comes into play for higher-beam intensities and results in a deviation of the beam's trajectory in the direction of the externally applied electric field, which is commonly denoted as bending [19]. As a consequence, the less intense innermost hump bends less to the left during propagation.

Finally, we investigate the question wether it is possible to generate a vector soliton consisting of a combination of two higher-order modes without the fundamental Gaussian mode. Although, a successful self trapping of a double- and triple-humped structure has been reported in the planar geometry [5], it has never been observed in the $(2+1)$D configuration before. To generate such a configuration, we derive a double- and a triple-humped mode beam from our laser with the help of several beam splitters and mirrors mounted on piezo-electric elements. Each higher-order mode constitutes of two or three mutually coherent and parallelly propagating beams, respectively. The reflection of one component from an oscillating mirror destroys the coherence in the same way as described above. The triple- and double-humped beam are coupled into the crystal in such a way that the peaks of the dipole beam overlap with the dark notches of the THS. Both components are shown in the top and bottom row of Fig. 4, respectively.

The input intensity distribution is given in Figs. 4(a), while the result of the separate propagation of 13.5 mm in the 1.9 kV-biased crystal is shown in Figs. 4(b). Neither the THS ($P_{\mathrm{THS}}=2.2\ \mu$W) in the upper row nor the dipole ($P_{\mathrm{d}}=2.6\ \mu$W) underneath form a localized and nondiverging structure. The single lobes of both components repel each other during propagation due to the phase between neighboring lobes. The relative distance of the marginal beamlets of the THS increases from 80 μm at the input face to 175 μm at the output face, as well as the dipole peaks gain about 35 μm in distance while propagating through the nonlinear medium. The scenario changes drastically when both components copropagate simultaneously in the crystal. The vertical circumference of the triple-humped component reduces to 110 μm and the dipole's vertical distance gets even smaller than at the crystal's front face. Generally, both components maintain their transverse shape. The innermost peak of the triple-humped component gets elongated in the vertical direction [Fig. 4(c), top] as it basically traps the two beamlets of the dipole [Fig. 4(c), bottom] which in turn, trap the two marginal beamlets of the THS. So, the combination of both higher-order components forms a bound self-focused state whereas both constituents itself diverge during propagation. The mutual stabilization of these multihumped light structures reveals that it is possible to generate self-trapped optical beams with a complex internal structure even in the absence of a fundamental and nodeless Gaussian beam. Due to the limited dimensions of our crystal and the restriction to two observation planes at $z=5$ and 13.5 mm statements about the stability and the propagation behavior of these solitary waves are not very reliable and will therefore be treated in the following theoretical section.

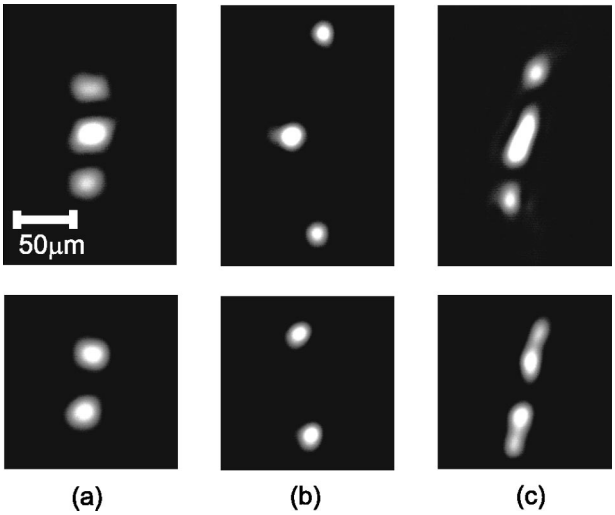

FIG. 4. Generation of a vector soliton from a double-triple-humped pair. (a) input intensity distributions, (b) output after a separate propagation of 13.5 mm, and (c) both components copropagating.

III. THEORY

Here, we investigate the propagation of higher-order modes in an anisotropic nonlinear medium numerically to support and extend the results of the experiments described above. The propagation of two mutually incoherent beams in a photorefractive medium may be described by the paraxial approximation for optical beams [18]

$$\frac{i\partial}{\partial z}A_{1,2}+\frac{1}{2}\Delta_{\perp}A_{1,2}=\frac{\gamma}{2}\left(E_0-\frac{\partial\varphi}{\partial x}\right)A_{1,2}, \qquad (1)$$

where $A_{1,2}$ represents the slowly varying amplitude of the two optical fields. z is the direction of propagation, $\Delta_\perp$ represents the transverse Laplacian $(\partial^2/\partial x^2+\partial^2/\partial y^2)$, and φ describes the material's electrostatic potential induced by the two beams. $\gamma=k^2n_0^2w^2r_{\rm eff}$ is the coupling constant, k is the wave number, n_0 is the material's ordinary refractive index, w is the beam waist at the crystal's front face, and $r_{\rm eff}$ represents the effective electro-optic coefficient. The transverse coordinates x and y are scaled by the beam waist w and the propagation coordinate z is scaled by the diffraction length $L_D=knw^2$. With typical beam waist parameters of 10–12 μm and an ordinary refractive index of SBN of $n=2.3$ a single diffraction length is equivalent to 3–4 mm in the real physical system. The electrostatic potential φ is given by a material equation derived from the Kukhtarev model for a photorefractive nonlinearity [13]

$$\nabla^2\varphi=-\nabla\varphi\nabla\ln I+E_0\frac{\partial}{\partial x}\ln I. \tag{2}$$

Here, the normalized intensity $I=1+|A_1|^2+|A_2|^2$ is given in units of the saturation intensity, and E_0 describes the external electric field that is applied in the horizontal transverse x direction. The diffusion of the charge carriers that is small compared to the drift effect due to the external electric field is neglected here. The system of equations is not integrable and therefore no analytical solutions can be determined. Therefore, we restrict on the split-step Fourier method [21] and demonstrate the evolution of the beams within a parameter range comparable to the experimental conditions.

A. Numerical results

Figure 5 demonstrates the spatial evolution of a copropagating vortex beam $(m=2)$ and a fundamental Gaussian mode. Both mutually incoherent components are depicted separately in the upper and bottom row for different propagation distances with an applied voltage of 4.5 kV/cm. In Fig. 5(a), the input intensity is given. Figure 5(b) shows the evolution at $z=0.25$. The vortex component [Fig. 5(b), top] starts to disintegrate and develops two instead of one dark notch in its center, which is similar to the experimentally observed structure depicted in Fig. 2(a). When propagating further to $z=0.5$, the vortex beam transforms first into a two-peak-structure [Fig. 5(c), top] and later into a triple-humped component that lasts for several propagation lengths [Figs. 5(d)–5(f)]. This scenario was also observed in [16] for the case of a saturable nonlinear medium. Because of the initial screwlike transverse phase distribution of the vortex beam, the whole structure bears a nonvanishing angular momentum. In contrast to isotropic simulations presented in [10,16], we do not observe a smooth rotation of the higher-order component, but detect an angular oscillation around its central peak. This effect arises from the anisotropy of the model we used in our simulations. We never observe a horizontal orientation of the three beamlets. In anisotropic simulations, the induced refractive index change is negative at the horizontal margins of the light structures and acts in a defocusing way [22].Therefore, the THS will never align in the horizontal direction of the applied electric field.

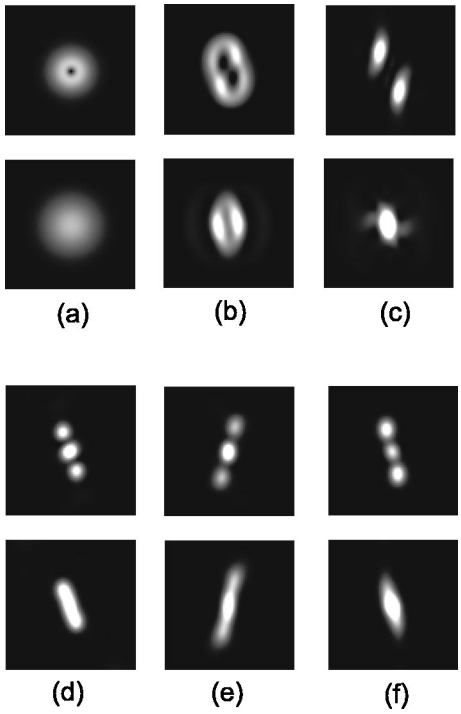

FIG. 5. Numerical simulation of a copropagating vortex component $(m=2)$ (upper row) with a fundamental Gaussian component (bottom row). Figs. (a)–(f) depict the transverse profiles for the propagation lengths: $z=0$; 0.25; 0.5; 2.75; 3.5; 4.

It is the influence of the fundamental Gaussian component that keeps the higher-order mode trapped during propagation, otherwise the vortex beam would completely disintegrate after a few diffraction lengths. It is only natural that the Gaussian component also becomes affected since both components have equal total power and jointly induce the multimode waveguide in which they both propagate. As a consequence, it becomes elliptically shaped in the direction of the THS axis [Figs. 5(d)–5(f), bottom row]. These numerical calculations are in qualitative agreement to the experimental results depicted in Figs. 1 and 2. The simulation of the vortex component in Fig. 5(b) and the experimental picture in Fig. 2(a) show almost identical results for a relatively short propagation length. In the case when both components propagate for a distance of 13.5 mm, which corresponds to about paper diffraction lengths in the numerical simulations, the experiment as well as the simulations reveal that the vortex component undergoes a transition into a THS with nonzero angular momentum. In the next step, we investigate numerically the formation of a triple-humped vector soliton consisting of a THS and a nodeless fundamental mode as already demonstrated experimentally in Fig. 3. The propagation behavior of the two incoherently coupled modes is depicted in Fig. 6. The single frames are arranged in a similar way as in Fig. 3. The input intensity distribution is given in Figs. 6(a) for the triple-humped (top) and the Gaussian component (bottom). The evolution after an independent propagation of two diffraction lengths $(z=2)$ is given in Fig. 6(b).

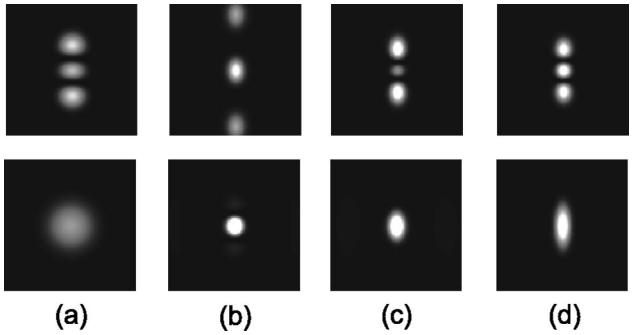

FIG. 6. Numerical simulation of the triple-humped vector soliton generation. Upper row, the THS, bottom row the fundamental Gaussian component with (a) input intensity distribution, beam evolution at $z=2$ for a separate propagation (b) and simultaneous propagation at $z=3$ (c) and $z=4$ (d).

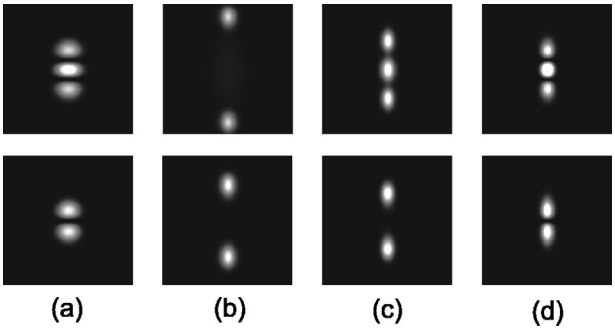

FIG. 7. Numerical simulation: The mutual stabilization of the two separating modes. Separate propagation of $z=2$ is given in (b). The copropagating modes for propagation lengths of $z=3$ (c) and $z=4$ (d).

It can be clearly seen that the three out-of-phase lobes of the higher-order component strongly repel each other during propagation [Fig. 6(b), top] and that the Gaussian mode forms an ordinary photorefractive soliton [Fig. 6(b), bottom]. The triple-humped mode itself does not form a self-trapped state as already demonstrated in the experiment in Fig. 3(b). The four frames in Figs. 6(c) and 6(d) demonstrate the trapping of the triple-humped mode at the propagation steps $z=3$ and 4 when it copropagates with the fundamental Gaussian beam. A comparison of the THS in (c) with the one depicted in (d) shows that the relative intensities of the three beamlets fluctuate during the propagation through the crystal. We infer that the initial intensity distribution is not an exact solution of Eqs. (1) and (2) but approximates a spatial vector soliton that is stable with respect to small amplitude deviations for at least ten diffraction lengths in propagation distance. Again, a complete agreement with the experimental results demonstrated in Fig. 3 is obvious.

To complete our investigations on higher-order mode vector solitons in saturable anisotropic media, we finally carry out some numerical simulations on the generation of a double- and a triple-humped vector soliton complex. Similar to the experiments and the numerical procedures described above, we combine a double-triple-humped pair of beams with equal total power in the nonlinear medium biased by an external voltage of 3.6 kV. Neither the dipole component nor the THS form a self-trapped state when propagating separately, as already demonstrated above. However, the incoherent coupling of both beams leads to the formation of a localized light structure. Figure 7 demonstrates the evolution of a triple-humped optical beam with two π-phase shifts in the upper row, and the dipole-mode beam in the bottom row [Fig. 7(a)]. In the case of an independent propagation, each component itself spreads in the transverse plane and does not form a localized state [Fig. 7(b)]. The initial intensity distribution of the triple-humped component varies slightly from the simulation depicted in Fig. 6. As a consequence, the innermost peak interferes destructively with the two marginal peaks after $z=2$. It is the incoherent combination of the two modes that finally prevents the repulsion of the single beamlets as demonstrated in Figs. 7 (c) and 7(d) for propagation distances of $z=3$ and 4. Again, the theoretical simulations are in a qualitative agreement compared with the experimentally observed structures depicted in Fig. 4. Since we start from arbitrary initial conditions for the distance and relative intensity of the single lobes, the propagation of the two components comes along with strong fluctuations in intensity and distance. Our simulations, as well as our experimental investigations, demonstrate the general effect of mutual stabilization of the two components, but the shape of the components retains only for relatively short propagation distances of $z \approx 5$. Exceeding this typical distance, the fluctuations in relative intensity and distance increase remarkably and the triple-humped structure decays into a single-humped one, which finally traps the two lobes of the dipole component. A propagation distance of five diffraction lengths is beyond our experimental limit, and therefore the breakup could only be seen in the numerical simulations. Deriving a numerical solution for the initial beam profiles from the Eqs. (1) and (2), one might find stationary solutions for double-triple humped multicomponent solitary waves. A promising numerical procedure is the one proposed by Zozulya *et al.* and Petviashvili [20,23], but its application is beyond the scope of the work presented here.

IV. CONCLUSIONS

In conclusion, we have demonstrated the generation of higher-order mode vector solitons in a bulk saturable anisotropic nonlinear medium experimentally and numerically. We have shown that an optical vortex with a topological charge of $m=2$ is unstable and undergoes a transition into a triple-humped light structure when copropagating with a mutual incoherent Gaussian beam of equal total power. The beams interact only due to the non-local response of the material that is essential for the generation of these triple-humped structures. Additionally, we demonstrate that once a THS structure forms, it remains as a component of a stable vector soliton. Finally, it is even possible to generate a nondiverging light structure consisting of two higher-order modes that display a diverging propagation behavior when propagating separately. The mutual self trapping can be observed at least for a considerable propagation distance before the composite self-trapped light structures may disintegrate.

ACKNOWLEDGMENTS

We acknowledge support from S. Stankovic and Professor Tschudi, Darmstadt University of Technology, from the Deutsche Forschungsgemeinschaft under Project No. Ka 708/1-1, and the Fazit Foundation. Additionally we would like to thank Yuri S. Kivshar and Wieslaw Królikowski for helpful discussions.

[1] For an overview, see G.I. Stegeman and M. Segev, Science **286**, 1518 (1999).
[2] S.V. Manakov, Zh. Éksp. Teor. Fiz. **65**, 505 (1973) [Sov. Phys. JETP **38**, 248 (1974)].
[3] J.U. Kang, G.I. Stegeman, J.S. Aitchison, and N. Akhmediev, Phys. Rev. Lett. **76**, 3699 (1996).
[4] A.W. Snyder, D.J. Mitchell, and Y.S. Kivshar, Mod. Phys. Lett. B **9**, 1479 (1995).
[5] M. Mitchell, M. Segev, and D.N. Christodoulides, Phys. Rev. Lett. **80**, 4657 (1998).
[6] E.A. Ostrovskaya, Yu.S. Kivshar, D.V. Skryabin, and W.J. Firth, Phys. Rev. Lett. **83**, 296 (1999); E.A. Ostrovskaya and Yu.S. Kivshar, J. Opt. B: Quantum Semiclassical Opt. **1**, 77 (1999).
[7] W. Królikowski, N. Akhmediev, and B. Luther-Davies, Phys. Rev. E **59**, 4654 (1999).
[8] C. Anastassiou, M. Segev, K. Steiglitz, J.A. Giordmaine, M. Mitchell, M.F. Shih, S. Lan, and J. Martin, Phys. Rev. Lett. **83**, 2332 (1999).
[9] Z.H. Musslimani, M. Segev, D.N. Christodoulides, and M. Soljacic, Phys. Rev. Lett. **84**, 1164 (2000); Z.H. Musslimani, M. Segev, and D.N. Christodoulides, Opt. Lett. **25**, 61 (2000).
[10] J.J. García-Ripoll, V.M. Pérez-García, E.A. Ostrovskaya, and Yu.S. Kivshar, Phys. Rev. Lett. **85**, 82 (2000).
[11] W. Królikowski, E.A. Ostrovskaya, C. Weilnau, M. Geisser, G. McCarthy, Yu.S. Kivshar, C. Denz, and B. Luther-Davies, Phys. Rev. Lett. **85**, 1424 (2000).
[12] T. Carmon, C. Anastassiou, S. Lan, D. Kip, Z.H. Musslimani, and M. Segev, Opt. Lett. **25**, 1113 (2000).
[13] A.A. Zozulya and D.Z. Anderson, Phys. Rev. A **51**, 1520 (1995).
[14] D.V. Skryabin and W.J. Firth, Phys. Rev. E **58**, 3916 (1998).
[15] A.V. Mamaev, M. Saffman, and A.A. Zozulya, Phys. Rev. Lett. **78**, 2108 (1997).
[16] V. Tikhonenko, J. Christou, and B. Luther-Davies, Phys. Rev. Lett. **76**, 2698 (1996).
[17] A.V. Buryak, Yu.S. Kivshar, M.F. Shih, and M. Segev, Phys. Rev. Lett. **82**, 81 (1999).
[18] A. Stepken, M.R. Belić, F. Kaiser, W. Królikowski, and B. Luther-Davies, Phys. Rev. Lett. **82**, 540 (1999).
[19] J. Petter, C. Weilnau, C. Denz, A. Stepken, and F. Kaiser, Opt. Commun. **170**, 129 (1999).
[20] A.A. Zozulya, D.Z. Anderson, A.V. Mamaev, and M. Saffman, Phys. Rev. A **57**, 522 (1998).
[21] T. Taha and M.J. Ablowitz, J. Comp. Physiol. **55**, 203 (1994).
[22] W. Królikowski, M. Saffman, B. Luther-Davies, and C. Denz, Phys. Rev. Lett. **80**, 3240 (1998).
[23] I.V. Petviashvili, Fiz. Plazmy **2**, 469 (1976) [Sov. J. Plasma Phys. **2**, 257 (1976)].